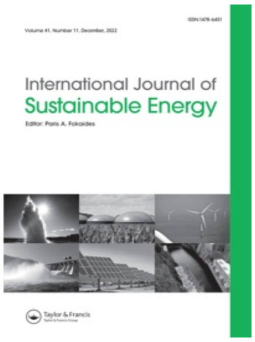

International Journal of Sustainable Energy

ISSN: (Print) (Online) Journal homepage: www.tandfonline.com/journals/gsol20

Performance simulation and analysis of a solar-assisted multifunctional heat pump system for residential buildings

Weimin Wang & Amirahmad Zare

To cite this article: Weimin Wang & Amirahmad Zare (2024) Performance simulation and analysis of a solar-assisted multifunctional heat pump system for residential buildings, International Journal of Sustainable Energy, 43:1, 2394116, DOI: 10.1080/14786451.2024.2394116

To link to this article: https://doi.org/10.1080/14786451.2024.2394116

Published online: 21 Aug 2024.

INTERNATIONAL JOURNAL OF SUSTAINABLE ENERGY
2024, VOL. 43, NO. 1, 2394116
https://doi.org/10.1080/14786451.2024.2394116

Taylor & Francis
Taylor & Francis Group

OPEN ACCESS

Check for updates

Performance simulation and analysis of a solar-assisted multifunctional heat pump system for residential buildings

Weimin Wang[a] and Amirahmad Zare[b]

[a]Department of Engineering Technology, University of North Carolina at Charlotte, Charlotte, NC, USA; [b]Department of Mechanical Engineering and Engineering Science, University of North Carolina at Charlotte, Charlotte, NC, USA

ABSTRACT

As building electrification is recognised as an important opportunity to reduce greenhouse gas emissions, the integration of solar energy and heat pump represents a promising solution towards net-zero carbon buildings. This paper presents a hybrid multifunctional solar-assisted heat pump (SAHP) system that can provide space heating, space cooling, domestic hot water, and onsite electricity generation. Photovoltaic-thermal collectors are used for electricity generation, heat collection, and radiative cooling. The system design and controls support fourteen operational modes involving different components. TRNSYS software is used to model and simulate the multifunctional SAHP system. With a 2-m^3 storage tank and 30-m^2 PVT collectors, the multifunctional SAHP system has a seasonal performance factor of 2.7 in Baltimore and 3.7 in Las Vegas. The onsite electricity generation can cover 53% of the building's electricity needs in Baltimore and 83% in Las Vegas.

ARTICLE HISTORY
Received 17 June 2024
Accepted 12 August 2024

KEYWORDS
Photovoltaic-thermal collectors; heat pump; TRNSYS; building simulation; thermal storage

Nomenclature

AEC	annual electricity savings ($)
b_0	incidence angle modifier coefficient
$CC_{MaxDiff}$	maximum acceptable capital cost difference ($)
E	electricity consumption or generation (J)
$f_{sol,el}^{sys}$	system solar electrical fraction
$f_{sol,el}^{site}$	site solar electrical fraction
G_T	solar irradiance on the collector surface (W/m^2)
h_r	radiative heat transfer coefficient (W/m^2-°C)
$K_{\tau\alpha}$	incidence angle modifier
PercentCredit	incentives in percentage of the capital cost (%)
Q	thermal energy (J)
R	thermal resistance (°C/W)
S	absorbed solar radiation (W)
SPP	simple payback period (yr)
T	temperature
β_T	the temperature coefficient of PV electrical efficiency (1/°C)
β_G	the radiation coefficient of PV electrical efficiency (m^2/W)
ϵ	PV surface emissivity
η	efficiency

CONTACT Weimin Wang weimin.wang@uncc.edu

θ	angle of incidence (°)
ρ	PV module surface reflectance
σ	Stefan-Boltzmann constant
$\tau\alpha$	the solar transmittance-absorptance product of PV module cover

Subscripts

a	ambient air
abs	absorber plate
avg	average
bot	bottom
col	PVT collector
coolingSP	cooling setpoint temperature.
e	electricity
heatingSP	heating setpoint temperature
high	high temperature limit
in	inlet
low	low temperature limit
n	normal incidence
out	outlet
PV	photovoltaic solar cell
space	building space air
*sp*1	the low temperature limit of the liquid used directly for space heating
*sp*2	the low temperature limit of the liquid used for the heat pump source
*sp*3	the high temperature limit of the liquid used directly for space cooling
STC	standard test conditions
sys	system
*tk*1	thermal storage tank
*tk*2	domestic hot water tank
top	tank top

Abbreviations

AC	alternating current
ASHP	air-source heat pump
CDD	cooling degree day
COP	coefficient of performance
DHW	domestic hot water
HDD	heating degree day
HP	heat pump
PV	photovoltaic
PVT	photovoltaic thermal
SAHP	solar-assisted heat pump
SC	space cooling
SH	space heating
SPF	seasonal performance factor
TSG	thermal storage tank

1. Introduction

The building sector consumes the most energy in many countries of the world. In the U.S., buildings account for 40% of the total primary energy use: 22% from residential buildings and 18% from commercial buildings (EIA 2022). For residential buildings, space heating, domestic hot water (DHW), and space cooling are three major energy end uses, which respectively contribute to 43%, 19%, and 8% of the total energy consumed by the residential sector. Currently, 88% of the energy consumed by residential buildings in the U.S. is from fossil fuels (EIA 2022). Because fossil fuels are non-renewable resources and the combustion of fossil fuels emits greenhouse gases, efforts are needed to switch from fossil fuels to renewable energy to meet the demands of people.

Building electrification represents an important opportunity towards decarbonising the U.S. economy by 2050. Replacing fossil fuel-based heating equipment with efficient heat pumps can significantly reduce energy consumption in residential buildings and address fossil fuel-associated environmental concerns. In this respect, geothermal heat pumps, ductless mini-split heat pumps, solar-assisted heat pumps, and heat pump water heaters are all promising technologies to be considered in the process of building electrification.

Traditionally, air-source heat pumps and solar collectors are used separately to reduce the primary energy consumption in residential buildings, where the heat pump is used for space heating and cooling while the solar collectors are used for DHW heating. The decoupling of heat pump and solar collectors has operational drawbacks when the air temperature is low in winter. First, both the capacity and coefficient of performance (COP) of the heat pump decrease with the outdoor air temperature. Thus, the capacity may become insufficient to meet the heating load, which triggers the use of auxiliary electrical heating. Particularly, many old-fashioned heat pumps have the cut-off ambient air temperature at as high as – 5°C, below which the heat pump no longer operates. Second, as for solar heating, the solar collectors cannot be used directly for DHW when the daily solar radiation is low, which in turn leads to a low solar utilisation ratio. Coupling solar collectors with the heat pump can complement each other to achieve high solar utilisation and high COP of the heat pump. The solar collectors coupled with the heat pump can be conventional solar thermal collectors and hybrid photovoltaic-thermal (PVT) collectors (Mohanraj et al. 2018). In SAHP systems, the heat pump's COP is improved due to the boosted evaporator temperature. Meanwhile, when coupled to the heat pump, the solar collectors have a low operating temperature, leading to the increase of solar fraction (Bakker et al. 2005; Banister and Collins 2015). If PVT collectors are used, the low operating collector temperature is also beneficial to the PV module's electrical efficiency. With efforts on high performance and even net-zero energy buildings, SAHP systems have attracted increasing attention in recent years, as demonstrated by the two task forces (Task 44 and Task 60) of the Solar Heating & Cooling Programme under the International Energy Agency. Badiei et al. (2020) provided a chronological review of advances in solar-assisted heat pump technology.

The literature has numerous studies on residential SAHP systems for DHW generation (e.g. Banister and Collins 2015; Li and Huang 2022; Qu et al. 2015; Sterling and Collins 2012), space heating (e.g. Del Amo et al. 2020; Ma et al. 2021; Vallati et al. 2019), and the dual purposes of space heating and DHW (e.g. Hadorn 2015; Martinez-Gracia et al. 2022; Simonetti et al. 2020). By expanding the functionality to include space cooling, a multifunctional SAHP system can be developed.

Chu et al. (2014) presented a multifunctional SAHP system for space heating, space cooling, dehumidification, and DHW in a high-performance house. The SAHP system consisted of conventional solar collectors, two thermal storage tanks, and a liquid-to-liquid heat pump. An air-handling unit was used to heat, cool, and dehumidify the supply air. In the winter, the cold tank was charged with the solar collectors and used as the heat pump's source to maintain the temperature at the bottom of the hot water tank no less than 40°C. The water in the hot tank was used for DHW and space heating needs. In the summer, the heat pump operation was reversed to maintain the temperature at the top of the cold tank no greater than 6°C. To avoid overheating of the hot water tank in the summer, if the temperature at the bottom of the hot tank was above 40°C, the refrigerant flow would bypass the hot water tank, and the heat would be dissipated to the ambient via an outdoor radiator. Therefore, the heat pump had two cooling sources (i.e. hot water tank and ambient air) in summer.

Wang et al. (2011) presented a dual-source multifunctional SAHP system for space heating, space cooling, and DHW heating. The system had seven operational modes. An experimental setup was built to verify the system could work in all seven operational modes. However, no details were given on how to determine which source should be used at what conditions. In addition, it is not clear whether the water tank had an auxiliary heating device to maintain the tank temperature setpoint.

Cai et al. (2016; 2017) proposed and studied the operation of a dual-source multifunctional heat pump system for space heating, space cooling, and DHW. The system could support the following five operational modes: (1) air source for DHW heating, (2) solar water source for DHW heating, (3) air source for space heating, (4) solar water source for DHW heating, and (5) air source for space cooling. They developed a numerical model for the system and verified the model with laboratory tests. Through simulations, Cai et al. (2017) found that using the air source was superior to the solar water source for space heating when the ambient temperature was above 4°C, and the solar water source was more efficient for DHW heating when the ambient temperature was below 3°C.

Entchev et al. (2014) proposed a solar-assisted ground source heat pump system for space heating, space cooling, DHW, and electricity generation. The system consisted of PVT collectors, a solar tank, a hot-water tank, a cold-water tank, and a ground source heat pump with boreholes. The solar tank was used to preheat the city water and transfer heat energy to the hot-water tank at applicable conditions. The hot-water tank had two immersed heat exchangers for space heating and DHW. The cold-water tank was used to provide chilled water for cooling in the summer season. The ground source heat pump was equipped with a desuperheater to preheat the city water for DHW use. The SAHP system was compared with a reference system having a boiler and a chiller for space conditioning and DHW in Ottawa, Canada. TRNSYS simulation results showed that the multifunctional SAHP system had 58% energy saving than the reference system.

Besagni et al. (2019) experimentally investigated a multifunctional SAHP system for a detached house in Milan, Italy. The SAHP system had PVT collectors, a DHW tank, an intermediate-temperature storage tank used as the water source of the heat pump, an intermediate storage tank used to provide water to fan coils, and a heat pump. The heat pump was equipped with an air-source evaporator and a water-source evaporator connected in series to provide space heating, space cooling, and DHW. Besagni et al. estimated that their SAHP system had 15.4% lower daily-averaged energy consumption than the baseline air-to-water heat pump system. A follow-up study (Leonforte et al. 2022) improved the system design and operation with two changes (1) the PVT collectors were directly connected to the source side of the heat pump instead of indirect connection via the storage tank, and (2) for space heating, the collectors and the ambient air were employed simultaneously instead of alternatively.

Based on the reviewed multifunctional SAHP systems, it can be found that the functionality of space cooling has been mostly achieved with the use of dual-source heat pumps. When the heat pump operates for space cooling, either the ambient air or the ground is used as the cooling source. PVT collectors can be used for radiative cooling as well. Several studies (Eicker and Dalibard 2011; Fiorentini, Cooper, and Ma 2015; Gürlich, Dalibard, and Eicker 2017; Lin et al. 2014), either numerical or experimental, have been performed to estimate the nighttime radiative cooling potential of PVT collectors. These studies did not investigate the use of PVT collectors as an integrated component of SAHP systems. Coupling radiative cooling of PVT collectors with heat pump seems to be a promising approach because (1) the radiative cooling power is low and dependent on climate conditions; and (2) the approach shares the similar principle of SAHP for heating. However, no research has been found on the development of a multifunctional SAHP system that leverages PVT collectors for space cooling. In addition, there is a lack of comprehensive analysis of operational modes for multifunctional SAHP systems (e.g. what modes are possible and which ones are important). This research aims to fill in the knowledge gap by proposing a novel multifunctional SAHP system and evaluating its performance with TRNSYS simulations. The major contributions of this work include the following:

- PVT collectors are used to serve three functions, including electricity generation (daytime), heat collection (usually daytime) in the heating season, and radiative cooling (usually nighttime) in the cooling season. Compared with the literature that uses PVT collectors for electricity generation or heat collection, the concept of SAHP system design and operation based on radiative cooling is new.

- The system design supports a comprehensive list of fourteen representative operational modes for SAHP systems. The results of system running time in those operational modes are important to guide future research on system design optimisation and simplification in different climate conditions.
- This work originally includes an operational mode that uses heat pump to charge hot water storage. This unique operational mode has been demonstrated to be beneficial for the system performance through TRNSYS simulation.

2. System design and operation

2.1. System design

Figure 1 shows the schematic of the multifunctional solar-assisted heat pump system design. Major components of the system include unglazed PVT collectors, a liquid-to-liquid heat pump, a thermal

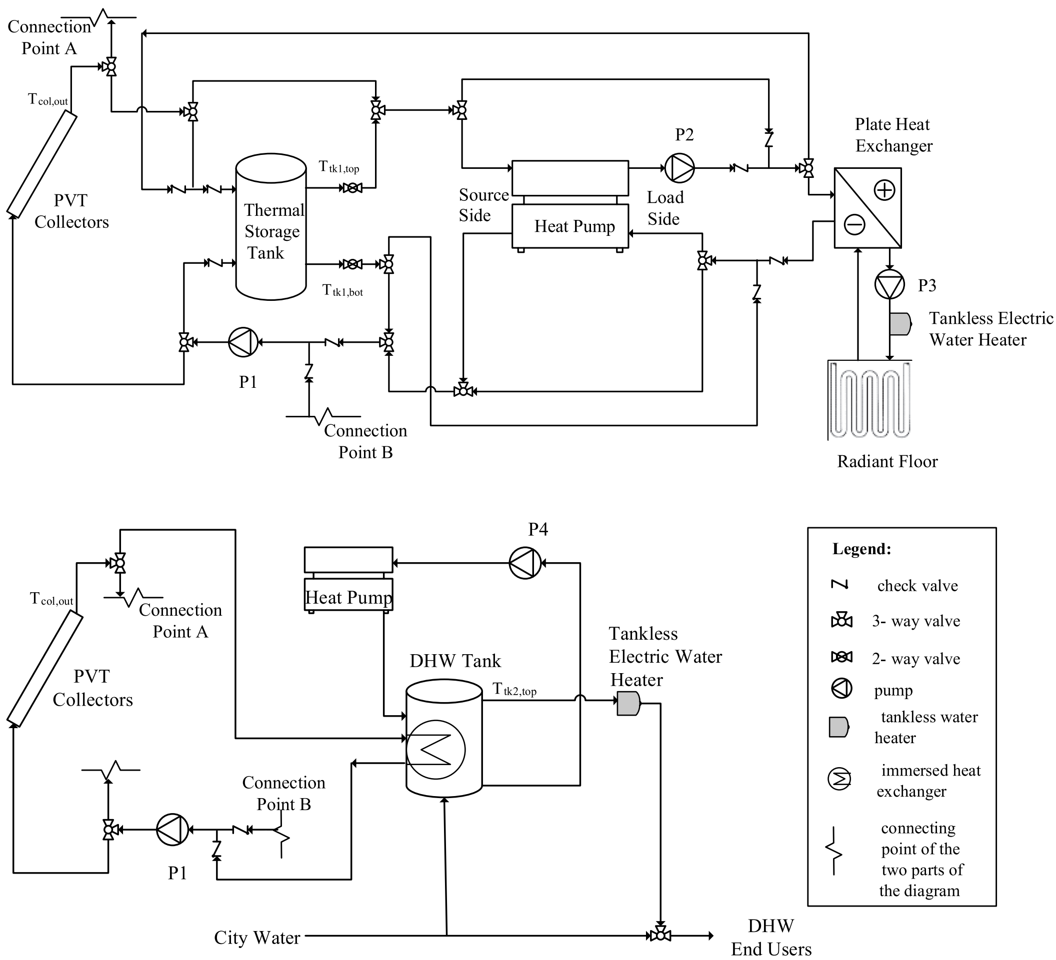

Figure 1. Schematic diagram of the studied multifunctional SAHP system: the upper part for space conditioning and the lower part for DHW production.

storage tank for space conditioning, a DHW tank, two instantaneous electric water heaters (one for space heating and another for DHW production), four circulating pumps, and a number of valves for flow direction controls. Because of the need for freezing protection in cold climates, a mixture of propylene glycol and water is used as the heat transfer medium between the PVT collectors, the storage tanks, and the heat pump. Though it is possible to circulate glycol solution directly through the plastic tubes embedded in the floor, a plate heat exchanger is used between the PVT-HP plant and the radiant floor, which has both positive and negative impacts. The advantage comes from the reduction of pressure drop across the radiant floor as water is less viscous than glycol. On the other hand, using the heat exchanger introduces effectiveness losses.

There exist different types of PVT collectors. Unglazed flat PVT collectors are used in this study because they not only serve the purpose of solar energy collection for heating but also act as radiative cooling panels to dissipate thermal energy to the sky in the cooling season, for which glazed collectors are not favourable (Eicker and Dalibard 2011; Lämmle, Herrando, and Ryan 2020). In addition, the collectors are sometimes used in the system as a heat exchanger for convective heat transfer between the ambient air and the glycol solution. In this respect, unglazed PVT collectors are preferable to glazed ones. Unglazed PVT collectors can generate low-temperature water up to 50°C (Lämmle, Herrando, and Ryan 2020), which is a major reason behind the use of hydronic radiant floor systems in the building. Since it is not reasonable to expect the PVT collectors to fully meet the thermal load, a liquid-to-liquid heat pump is used. When the heat pump is used for space conditioning, its source side connects to either the PVT collectors or the thermal storage tank, and its load side connects to the radiant floor system via the heat exchanger. The DHW tank water is heated by PVT collectors or the heat pump's desuperheater. The desuperheater uses superheated gases from the heat pump's compressor to heat the water circulated from the DHW tank. In addition, an instantaneous electric heater is placed after the DHW tank to ensure the hot water temperature has reached 49°C before being tempered with the city water.

2.2. Sequence of system operation

The seemingly complex piping (Figure 1) results from the system's high flexibility to support many operational modes. Figure 2 sketches the sequence of system operation. All operational modes are briefly described in this subsection.

Mode 1: PVT collectors for space heating. In this mode, Pump P1 is on, and it drives the glycol solution flowing from the PVT collectors to the plate heat exchanger. Mode 1 operates when (1) the space calls for heating, (2) the glycol outlet temperature ($T_{col,out}$) from the PVT collectors is greater than the temperature limit (T_{sp1}) acceptable for space heating, and (3) $T_{col,out}$ is greater than the thermal storage tank's top outlet temperature ($T_{tk1,top}$, see Figure 1). The third condition is used because the system has two alternative sources (PVT collectors and the storage tank), and the source with a higher temperature is applied first.

Mode 2: Thermal storage tank for space heating. In this mode, Pump P1 is on, and it drives the glycol solution flowing from the thermal storage tank to the plate heat exchanger. Mode 2 operates when (1) the space calls for heating, (2) $T_{tk1,top} > T_{sp1}$, and (3) $T_{tk1,top} > T_{col,out}$.

Mode 3: PVT-HP for space heating. In this mode, Pump P1 circulates the glycol solution between the collectors and the heat pump, while Pump P2 circulates the glycol between the heat pump and the plate heat exchanger. Because PVT collectors are located on the source side of the heat pump, the low temperature of the glycol from the heat pump's evaporator enhances solar utilisation. Mode 3 operates when (1) the space calls for heating, (2) $T_{sp1} \geq T_{col,out} > T_{tk1,top}$, and (3) $T_{col,out}$ is greater than the low-temperature limit (T_{sp2}) for heat pump running. It is worth noting that this mode works independently of solar radiation. At times of no solar radiation (e.g. cloudy days and nights), the collectors simply play the role of a convective heat exchanger to transfer energy from the ambient air to the glycol solution.

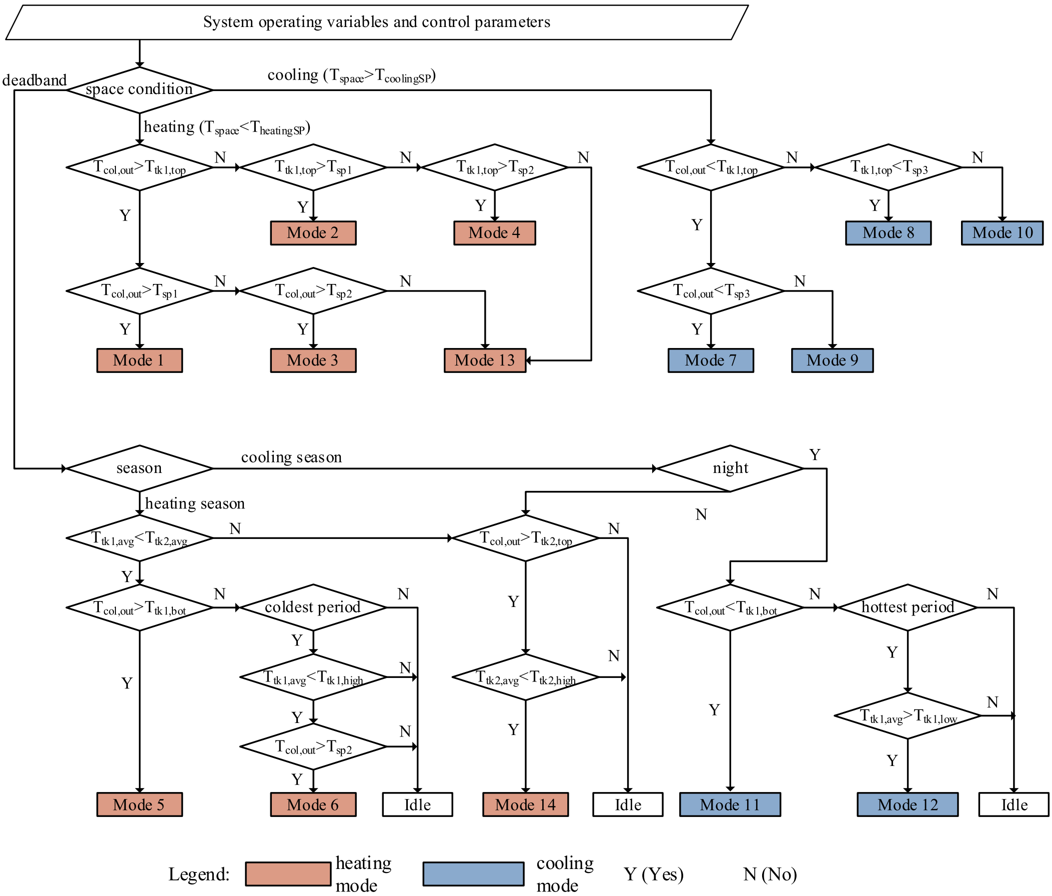

Figure 2. Flowchart diagram showing the system control sequence.

Mode 4: Tank-HP for space heating. In contrast to Mode 3, this mode uses the thermal storage tank as the heat pump's source. Mode 4 operates when (1) the space calls for heating, (2) $T_{sp1} \geq T_{tk1,top} > T_{col,out}$, and (3) $T_{tk1,top} > T_{sp2}$.

Mode 5: PVT for storage tank water heating. This mode uses the collectors to charge the storage tank for heating. This mode operates when (1) the space does not call for heating, (2) the system runs in the heating season, (3) the thermal storage tank average temperature is lower than the DHW tank average temperature, and (4) $T_{col,out}$ is greater than the storage tank's bottom outlet temperature ($T_{tk1,bot}$, see Figure 1). The second condition is needed because the system has only one thermal storage tank that is used to store warm water in the heating season and cold water in the cooling season. Therefore, a seasonal changeover point is required to determine the usage of the storage tank.

Mode 6: PVT-HP for storage tank heating. In literature, it is common to use the storage tank as the source of the heat pump for heating, as described in Mode 4. To our best knowledge, the storage tank has never been charged by the heat pump in previous studies of solar-assisted heat pump systems. Mode 6 is proposed in our work for the following two reasons. Firstly, because the storage tank has a small capacity intended for daily cycling, the depletion of the tank (i.e. $T_{tk1,top} < T_{sp2}$) would occur in many days if Mode 5 was merely relied on for tank charging. Secondly, using collectors as the heat pump's source increases solar utilisation, as explained in Mode 3. Mode 6 is used under the following conditions: (1) $T_{col,out} > T_{sp2}$, (2) neither of Mode 1 to Mode 5 is activated, (3) the system runs in a predefined coldest period of time, and (4) the average tank water temperature ($T_{tk1,avg}$) is less than a high limit for heat pump charging ($T_{tk1,high}$). Note that in the third condition, the coldest period is only part of the heating season when the storage tank is likely depleted.

Mode 7: PVT collectors for space cooling. Having the same pump status and fluid paths as Mode 1, Mode 7 operates when (1) the space calls for cooling, (2) the glycol outlet temperature ($T_{col,out}$) from the PVT collectors is lower than the temperature limit (T_{sp3}) acceptable for space cooling, and (3) $T_{col,out}$ is lower than the thermal storage tank's top outlet temperature ($T_{tk1,top}$). The third condition is used because the system has two alternative sources (PVT collectors and the storage tank), and the source with a lower temperature is applied first for cooling.

Mode 8: Thermal storage tank for space cooling. Having the same pump status and fluid paths as Mode 2, Mode 8 operates when (1) the space calls for cooling, (2) $T_{tk1,top} < T_{sp3}$, and (3) $T_{tk1,top} < T_{col,out}$.

Mode 9: PVT-HP for space cooling. Having the same pump status and fluid paths as Mode 3, Mode 9 operates when (1) the space calls for cooling, and (2) $T_{sp3} \leq T_{col,out} < T_{tk1,top}$.

Mode 10: Tank-HP for space cooling. Having the same pump status and fluid paths as Mode 4, Mode 10 operates when (1) the space calls for cooling, and (2) $T_{sp3} \leq T_{tk1,top} < T_{col,out}$.

Mode 11: PVT for storage tank water cooling. This mode operates when (1) the space does not call for cooling, (2) it is the night time in the cooling season, and (3) $T_{col,out}$ is lower than the storage tank's bottom outlet temperature ($T_{tk1,bot}$, see Figure 1).

Mode 12: PVT-HP for storage tank cooling. The rational of having this mode is similar to that of Model 6. This mode is included here for the purpose of completeness. Mode 12 is used under the following conditions:(1) neither of Mode 7 to Mode 11 is activated, (2) the system runs in a predefined hottest period of time, and (3) the average tank water temperature ($T_{tk1,avg}$) is higher than a low limit for heat pump charging ($T_{tk1,low}$).

Mode 13: backup electric heater for space heating. This mode operates when the space calls for heating but neither PVT collectors (Mode 3) nor the storage tank (Mode 4) can be used as the source for space heating because of the low-temperature limit setting for the glycol entering the heat pump's evaporator.

Mode 14: PVT collectors for DHW heating. In this mode, the heated glycol solution flows through the immersed heat exchanger in the DHW tank to heat the cold makeup water from the city mains. Mode 14 operates when (1) PVT collectors are not used in any of the modes for space conditioning, (2) $T_{col,out}$ is greater than the DHW tank temperature at the glycol inlet ($T_{tk2,top}$), and (3) the DHW tank water average temperature ($T_{tk2,avg}$) is less than a predefined high limit ($T_{tk2,high}$), the purpose of which is to avoid overheating the DHW tank.

3. System simulation

There exist several widely used building energy simulation programmes. The TRNSYS software is selected for this research mainly because (1) the TRNSYS software has a rich library of validated

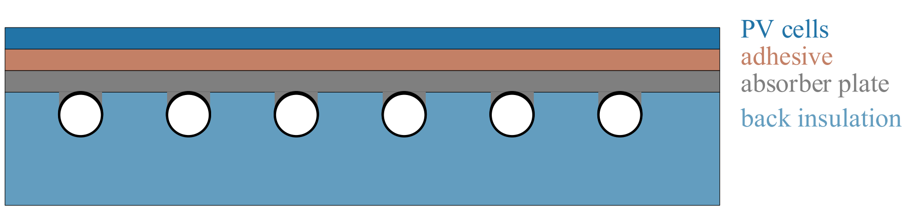

Figure 3. Schematic of unglazed sheet-and-tube PVT collector.

component models (e.g. solar collector, PV, and energy storage) commonly found in solar-based thermal and electrical energy systems, and (2) the TRNSYS software is featured with its open and modular structure, which facilities the creation of new components and the modification of existing components to simulate novel systems.

TRNSYS Type 560 is used to model PVT solar collectors. It establishes energy balance equations respectively for the PV cells, the absorber plate and the tube, and the fluid in the tube (Figure 3). Only equations related to PV cells are briefly presented here while a complete description of Type 560 can be found in Klein et al. (2018).

For the PV cells, the energy balance equation is written as:

$$S - h_c(T_{PV} - T_a) - h_r(T_{PV} - T_{sky}) - \frac{T_{PV} - T_{abs}}{R} = 0 \tag{1}$$

where, S is the absorbed solar radiation for thermal energy collection; T_{PV}, T_a, T_{sky}, and T_{abs} represent the cell temperature, the ambient air temperature, the effective sky temperature and the absorber plate temperature, respectively; h_c is the convective heat transfer coefficient between the PV cells and the ambient air; h_r is the radiative heat transfer coefficient between the PV cells and the sky; R is the thermal resistance of the adhesive layer, which is a user-defined parameter of the model.

In Equation 1, the absorbed solar radiation S is for thermal energy collection, after accounting for the solar energy used for electricity generation. Thus, S is expressed as:

$$S = (\tau\alpha)_n K_{\tau\alpha} G_T (1 - \eta_e) \tag{2}$$

where, $(\tau\alpha)_n$ is the solar transmittance-absorptance product of PV module at normal incidence, $K_{\tau\alpha}$ is the incidence angle modifier to consider the impact of incident angle on optical properties, G_T is the total solar radiation on the tilted collector surface, and η_e is the electrical efficiency of PV cells.

The value of $(\tau\alpha)_n$ in Equation 2 is determined from the PV reflectance, ρ, with $(\tau\alpha)_n = 1 - \rho$. The incidence angle modifier $K_{\tau\alpha}$ is based on the following equation:

$$K_{\tau\alpha} = \frac{(\tau\alpha)}{(\tau\alpha)_n} = 1 - b_0\left(\frac{1}{cos\theta} - 1\right) \tag{3}$$

where, θ is the angle of incidence and b_0 is a constant called the incidence angle modifier coefficient.

The electrical efficiency of PV is a function of the cell temperature and the incident solar radiation (Evangelisti, Guattari, and Asdrubali 2019):

$$\eta_e = \eta_{STC}[1 + \beta_T(T_{PV} - 25)][1 + \beta_G(G_T - 1000)] \tag{4}$$

where, η_{STC} is the PV efficiency at the Standard Test Conditions (cell temperature at 25°C and solar radiation at 1000 W/m^2), β_T and β_G refer to the temperature coefficient and the radiation coefficient of PV electrical efficiency, respectively.

In Equation 1, the radiative heat transfer coefficient is expressed as (Klein et al. 2018):

$$h_r = \varepsilon\sigma(T_{PV} + 273 + T_{sky} + 273)\{(T_{PV} + 273)^2 + (T_{sky} + 273)^2\} \tag{5}$$

where, ε is the PV surface emissivity, σ is the Stefan-Boltzmann constant, and T_{sky} is the effective sky temperature.

The effective sky temperature is a critical variable that could have a large impact on the system performance because of the consideration of radiative cooling. There are many sky temperature models (Evangelisti, Guattari, and Asdrubali 2019). TRNSYS Type 15, a component for weather data processing, is used to calculate the sky temperature. Type 15 calculates the effective sky temperature based on the model from Martin and Berdahl (1984).

Table 1 provides the parameters of unglazed PVT collectors used in this study. Nearly all these parameter values are from Grossule (2015).

Table 1. Parameters of unglazed PVT collectors.

Parameter	Value	Unit
Collector length	1.3	m
Collector width	1	m
Collector slope	45	degree
Absorber plate thickness	0.001	m
Absorber plate thermal conductivity	380	W/m-°C
Number of tubes	15	–
Tube diameter	0.036	m
Bond width	0.01	m
Bond thickness	0.001	m
Bond thermal conductivity	380	W/m-°C
Adhesive thermal resistance	0.001	m^2*°C/W
Back insulation thermal resistance	2.8	m^2*°C/W
PV surface reflectance	0.15	–
PV surface emissivity	0.89	–
Incident angle modifier coefficient	0.1	–
PV nominal electrical efficiency	0.184	–
Temperature coefficient of PV efficiency	−0.005	1/°C
Radiation coefficient of PV efficiency	0.00009	m^2/W

TRNSYS Type 927 is used to model the liquid-to-liquid heat pump via two external data files (one for heating and the other for cooling) that contain the catalog data for normalised capacity and normalised power consumption at different operating conditions (i.e. liquid flow rates and entering liquid temperature at both the source side and the load side). In this work, the catalog data are based on a 11.7-kW geothermal heat pump from WaterFurnace (model NSW040), which has its rated capacity and power consumption shown in Table 2. The original TRNSYS Type 927 was expanded to support the functionality of modelling desuperheater that uses superheated gases from the heat pump's compressor for hot water generation.

TRNSYS offers a number of component models (e.g. Types 39, 153, 156, etc.) for thermal storage using tanks. These models vary with respect to the number of ports (i.e. inlet and outlet), the number of immersed heat exchangers, and whether and what type of auxiliary heaters are supported. In our simulation model, TRNSYS Type 158 is used for the storage tank, and Type 156 is used for the DHW tank. Both tanks are cylindrical. The storage tank has two pairs of ports but no immersed heat exchangers. The DHW tank has one pair of ports for makeup water heating and another pair for connection to the heat pump desuperheater. Whenever there is hot water consumption at end use points, the cold water from city mains enters the DHW tank at the bottom and leaves the tank at the top. In contrast, the desuperheater-related ports have the opposite configuration. The DHW tank also has an immersed heat exchanger (i.e. a coiled tube) used to heat the water from PVT collectors when conditions permit. The heat exchanger is needed because glycol solution is used in the collector loop, but water is in the DHW tank.

To support the modelling of thermal stratification in this work, the tank volume was evenly divided into 6 vertical layers for both Type 156 and Type 158. Each layer, normally called a node, is assumed to be isothermal, and its energy balance is established by considering the following mechanisms: heat transfer between the tank and the ambient through the tank surfaces, fluid thermal condition between neighbouring nodes through nodes, fluid movement due to inlet and outlet flow streams, the heat convection between the tank fluid and the fluid in the immersed heat exchanger, and the mixing effects in case the nodes in the storage tank become thermally unstable.

Table 2. Parameters of the liquid-to-liquid heat pump.

Rating condition	Capacity (kW)	Energy efficiency ratio for cooling (W/W)	COP for heating (-)
Cooling (30°C source, 12°C load)	10.5	4.5	–
Heating (15°C source, 40°C load)	14.0	–	4.8

Table 3. Control parameters of the proposed system.

Control parameter	Value (°C)
T_{sp1}	30
T_{sp2}	−3
T_{sp3}	20
$T_{tk1,high}$	45
$T_{tk1,low}$	5
$T_{tk2,high}$	52
$T_{heatingSP}$	19
$T_{coolingSP}$	26

In addition to the above three TRNSYS Types for PVT collectors, the heat pump, and the storage tanks, other TRNSYS Types include Type 114 for pumps, Type 91 for the plate heat exchanger, Type 138 for the tankless water heaters. A full description of these models is not presented for the brevity of this paper. More details can be found in (Zare 2021).

A new TRNSYS type has been developed for controlling the system operation. This type determines the applicable operating mode based on the control sequence described in Section 2.2 and then determines the control signals of all diverters, pumps, and the heat pump corresponding to the operating mode. Table 3 lists the settings of control parameters.

4. Building and climate conditions

We used a hypothetical single-family house to investigate the system performance. The house has one floor with a total area of 200 m^2. The floor has a rectangular shape with an aspect ratio of 0.86. A slab-on-grade floor and wood-frame constructions are assumed. The house has a flat roof with a floor-to-ceiling height of 2.44 m. On each façade, windows occupy 2 m^2. The thermal performance of exterior building envelope meets the minimum code requirement of the International Energy Conservation Code for residential buildings (IECC 2006).

The climate affects solar radiation, building thermal loads, and radiative cooling. The operational modes discussed in Section 2.2 may play different roles, and the system performance is expected to vary in different climates. Therefore, this work considers two locations (i.e. Baltimore, MD, and Las Vegas, NV) with quite different climate conditions. Baltimore has a mixed climate, cold in winter and hot in summer, and it has annual heating degree days (HDDs) of 2495 °C-day and cooling degree days (CDDs) of 704 °C-day. In contrast, Las Vegas has a milder and dryer climate (HDDs = 1097 °C-day, CDDs = 1929 °C-day) (ASHRAE 2017). All degree days are calculated with a base temperature of 18.8°C. The heating season, the cooling season, and the shoulder season are defined with minor differences in Baltimore and Las Vegas, as Table 4 shows.

5. Simulation results and analysis

The results presented in this section are based on TRNSYS simulation with a two-minute time step and the typical meteorological year weather data (TMY-2) for the considered locations.

5.1. Verification of the control implementation

As seen from the sequence of operation described in Section 2.2, the SAHP system operates differently with weather conditions. The effort of verifying control implementation needs to cover all possible system operational modes. Therefore, a typical day was selected to represent each of the winter season, the summer season, and the shoulder season. For each typical day, the ambient temperature (T_a), the space air temperature (T_{space}), the PVT collector output temperature ($T_{col,out}$), the thermal storage tank output temperature ($T_{tk1,top}$) and the system operational modes were investigated to verify the system operation.

Table 4. Seasons defined in the two locations.

Location	Heating season	Cooling season	Shoulder season
Baltimore	November to April	June to September	May, October
Las Vegas	December to February	April to October	March, November

February 5 was selected as the day to represent the winter season in Baltimore, MA. As Figure 4 shows, at the beginning of the day, the space temperature was around 19°C. The system ran for space heating. According to the control sequence in Figure 2, Mode 4 (Tank-HP for space heating) was the operational mode used for space heating because (1) the storage tank output temperature ($T_{tk1,top}$) was higher than the collector outlet temperature $T_{col,out}$; and (2) $T_{tk1,top}$ was in between the temperature limits (T_{sp1} = 30°C and T_{sp2} = −3°C). Mode 4 continued until the space temperature (T_{space}) reached 19.5°C at around 2:30am when the system entered its idle mode. At about 6am, T_{space} dropped to 18.5°C and space heating was required again. Because the conditions for running Mode 4 were still satisfied, the heat pump used the storage tank as its source for space heating. Using Mode 4 led to the gradual decrease of the thermal storage tank temperature. At around 7am, $T_{tk1,top}$ dropped below T_{sp2}, which deactivated Mode 4 but activated Mode 13 (backup electric heater for space heating). Mode 13 was used until around 9am when the following conditions were met (1) $T_{col,out}$ was higher than $T_{tk1,top}$; and (2) $T_{col,out}$ was in between T_{sp1} and T_{sp2}. Thus, Mode 3 (PVT-HP for space heating) was activated, and this mode continuously ran until the space temperature reached 19.5°C at around 10am. At this time, because $T_{tk1,avg}$ was lower than $T_{tk2,avg}$ and $T_{col,out}$ was higher than $T_{tk1,bot}$, Mode 5 started to use PVT collectors directly for heating the storage tank. This mode ran continuously until around 2pm, when $T_{col,out}$ dropped below $T_{tk1,bot}$ and PVT collectors were no longer able to directly charge the thermal storage tank. During the period of running Mode 5 from 10am to 2:00pm, the storage tank temperature increased from – 3°C to 12°C. Because February was regarded as one of the coldest months, using the heat pump to charge the

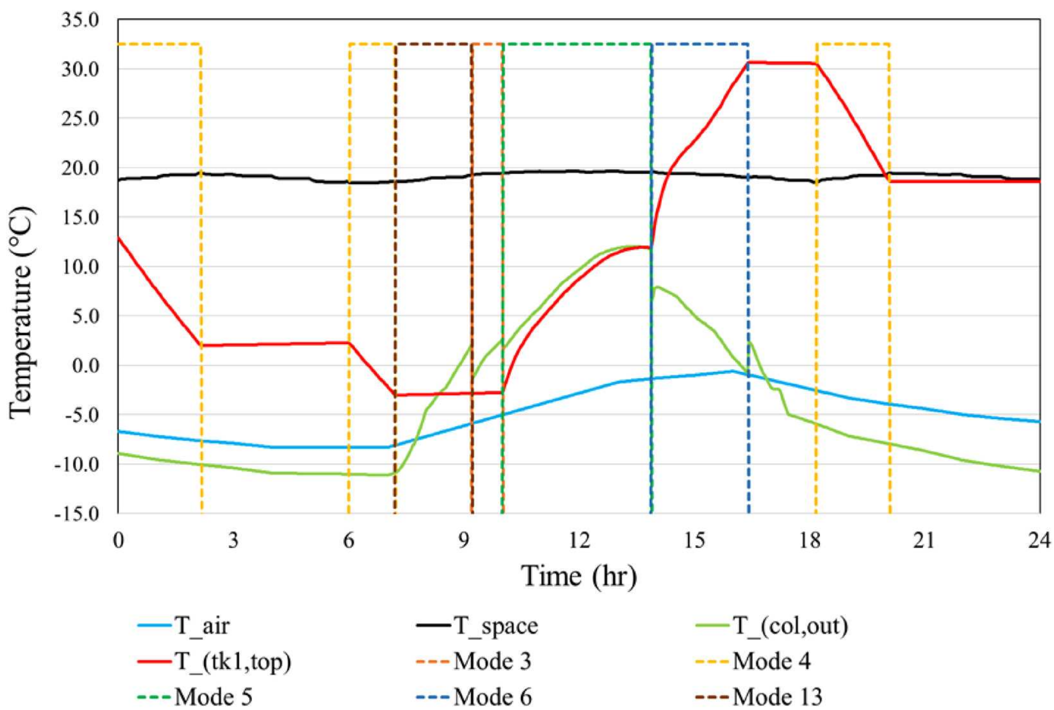

Figure 4. System operation on February 5 in Baltimore, MA.

storage tank with PVT collectors being the source (Mode 6) was then used until around 4:30pm when $T_{col,out}$ dropped below T_{sp2}. During the period of running Mode 6, the storage tank temperature increased from 12°C to 30°C. By comparing the trajectories of storage tank temperature between Mode 5 and Mode 6, one can find that the thermal storage was charged at a higher rate in Mode 6 because the heat pump provides a higher heating capacity than the collectors. After 4:30pm, the system was idle except for the period from 6pm to 8:30pm when Mode 4 was used for space heating.

Similarly, the implemented controls were verified for the other two days representing the summer season and the shoulder season.

5.2. Statistical analysis of system operational modes

Considering that the system has many possible operational modes, it is valuable to perform a statistical analysis of the running time of all modes in different months. Such a statistical analysis intends to set the foundation of simplifying controls for system operation in future.

Figures 5 and 6 are the stacked bar charts showing the hours of system operation in different modes for space heating and cooling in each month.

Of all modes related to space heating, Mode 1 (PVT-SH, PVT for space heating), Mode 2 (TSG-SH, Thermal storage tank for space heating), and Mode 3 (PVT-HP-SH, Heat pump for space heating with the PVT collectors being the source) played very minor roles because of their limited operation hours. Mode 1 was not used at all, demonstrating that unglazed plate PVT collectors can provide low-temperature heat only. In Baltimore, Mode 4 (TSG-HP-SH, Heat pump for space heating with the storage tank being the source), Mode 5 (PVT-TSG Heat, Storage charging with the PVT collectors), Mode 6 (PVT-HP-TSG Heat, Heat pump for storage charging with PVT collectors being the source), and Mode 13 (Backup heater) were predominately used. Note that Mode 6 was allowed only in the four coldest months (January, February, November, and December). In Las Vegas, both Mode 4 and Mode 5 were predominately used, while Mode 13 was occasionally used (5 hrs in January and not used in other months) because of the mild weather conditions.

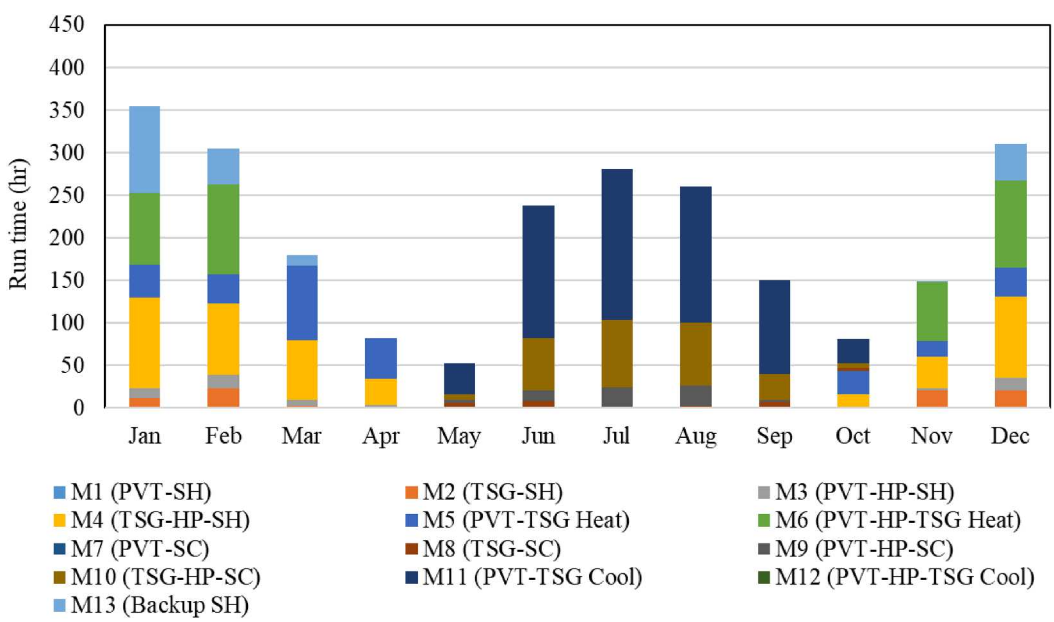

Figure 5. Monthly running time of different operational modes related to space conditioning in Baltimore, MA.

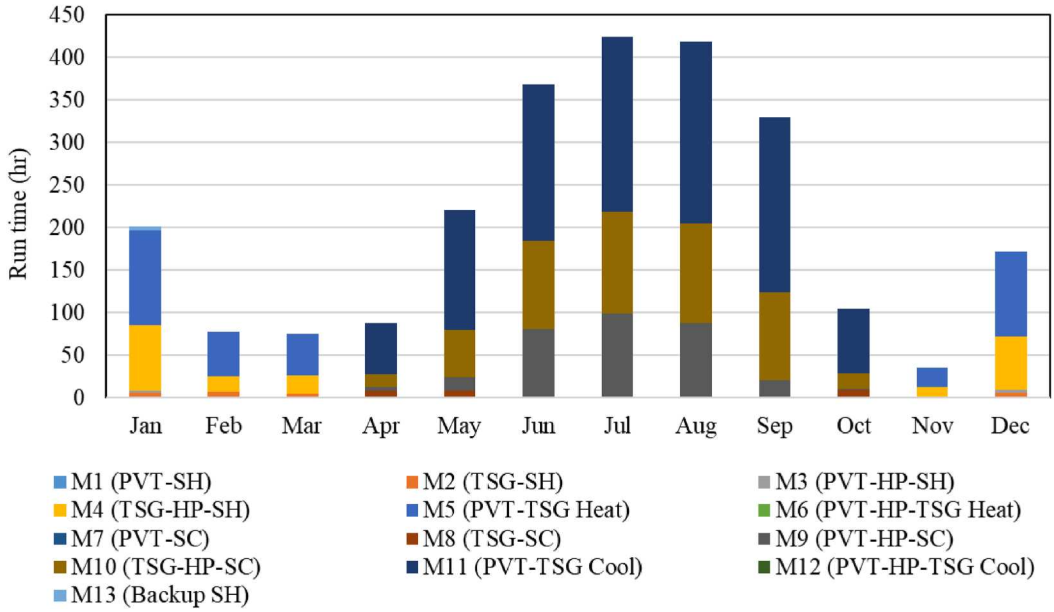

Figure 6. Monthly running time of different operational modes related to space conditioning in Las Vegas, NV.

Mode 6 was disabled because it did not contribute to energy savings, as will be further discussed later in Section 6.2.

Of all modes related to space cooling, Mode 7 (PVT-SC, PVT for space cooling) and Mode 8 (TSG-SC, Thermal storage tank for space cooling) were rarely used in both locations, while Mode 10 (TSG-HP-SC, Heat pump for space cooling with the storage tank being the source) and Mode 11 (PVT-TSG Cool, Storage charging with the PVT collectors) were predominately used. Mode 9 (PVT-HP-SC, Heat pump for space cooling with the PVT collectors being the source) usage was also significant in Las Vegas, but not in Baltimore. Note that Model 12 was disabled in both locations because it did not contribute to energy savings, as will be further discussed later in Section 6.2.

5.3. Seasonal performance factors

According to IEA SHC Task 60 (Zenhäusern 2020) and Task 44 (Hadorn 2015), Seasonal Performance Factor (SPF) is defined as the ratio between the amount of useful heat and/or cold (with positive sign) generation to the electricity consumption over a specified period of time. SPF can be defined over different system boundaries, but it is used for the whole SAHP system in this work. The amount of useful heat and cold energy generation are determined at the interfaces between the SAHP system and the distribution system to end uses. If energy losses of the heat distribution system are not considered, which is the case in this work, the amount of useful heat and cold energy is the energy delivered to the space for heating, cooling and DHW end users. The electricity consumption comes from all components of the whole system, such as the heat pump, the auxiliary heater, and the pumps. Thus, SPF is expressed as.

$$SPF = \frac{\int (Q_{SH} + Q_{SC} + Q_{DHW})dt}{\int E_{sys}dt} \tag{6}$$

where, Q_{SH}, Q_{SC}, and Q_{DHW} represents the energy (J) delivered by the system for space heating, space cooling, and DHW, respectively, E_{sys} is the electricity consumption (J) of the system.

To put the calculated SPF in context, a reference system was defined to have a split air-source heat pump (ASHP) system for space heating and cooling and an electric water heater for DHW production. Electric resistance was used as auxiliary space heating. The performance data of the ASHP were based on a commercial product with the rated capacity of 10.6 kW, rated energy efficiency ratio of 3.4 for cooling and rated COP of 3.6 for heating.

Figures 7 and 8 compare the SPFs between the reference system and the SAHP system, respectively, for the two locations. Both monthly and annual overall values are presented in the figures. Because the SPF can be understood as the system COP for space heating, cooling and DHW, the system with a higher SPF is more energy efficient. Major observations from Figures 7 and 8 include the following:

- The SAHP system had higher SPFs than the reference system throughout the year for both locations. Major factors contributing the higher performance of the multifunctional SAHP system include (1) using PVT collectors can elevate the source-side temperature of the heat pump in winter, which saves the energy used for heating relative to the air-source heat pump particularly in the cold climate; (2) radiative cooling can decrease the source-side temperature of the heat pump in summer, which saves the energy used for cooling relative to the air-source heat pump particularly in the hot climate; and (3) the use of desuperheater and PVT collectors can significantly save the energy for DHW heating.
- In Baltimore, the monthly SPF ranged from 1.87 (January) to 3.97 (June) for the SAHP system, while it was from 1.13 (January) to 1.87 (July) for the reference system. The annual SPF was 2.69 and 1.59, respectively, for the above two systems.
- In Las Vegas, the monthly SPF ranged from 3.24 (November) to 4.82 (October) for the SAHP system, while it was from 1.27 (April) to 2.13 (July) for the reference system. The annual SPF was 3.70 and 1.90, respectively, for the above two systems.

The annual SPF of 2.69 in Baltimore and 3.70 in Las Vegas lies in the range of those values reported in literature. Based on the review by Miglioli et al. (2023), PVT-integrated indirect-expansion SAHP systems had a reported SPF between 2.3 and 4.5.

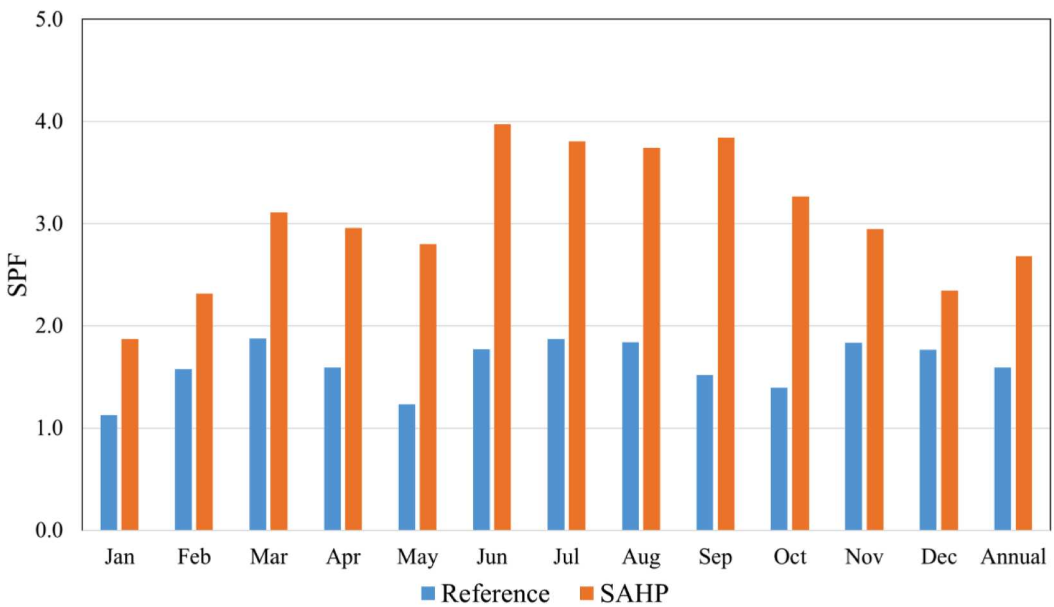

Figure 7. SPF comparison between the proposed and reference systems in Baltimore, MA.

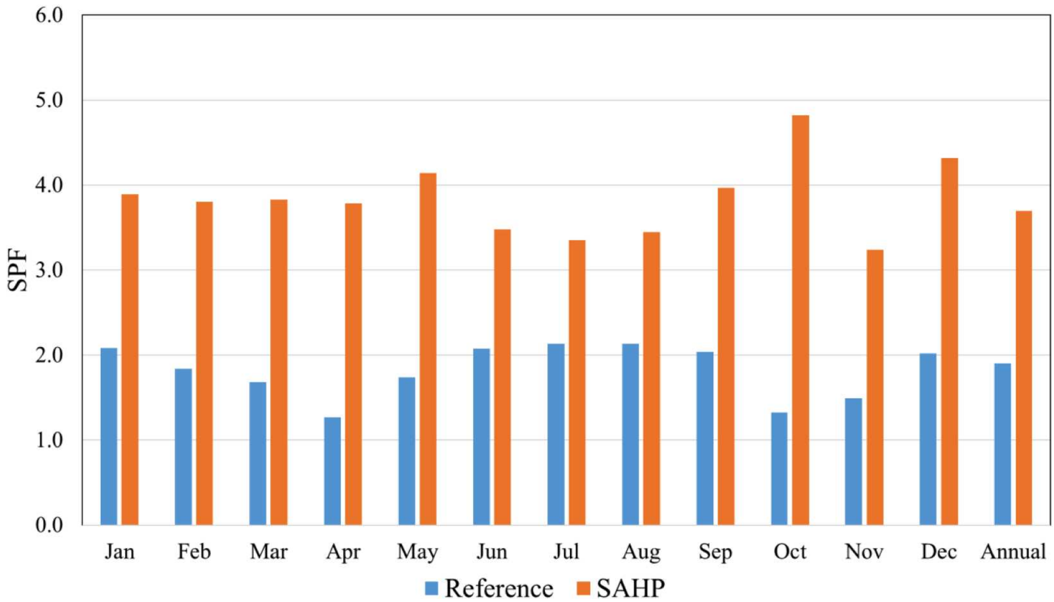

Figure 8. SPF comparison between the proposed and reference systems in Las Vegas, NV.

The metric of SPF considers the thermal aspect only. Because of the use of PVT collectors, the system also generates electricity, which is discussed next.

5.4. Solar electrical fraction

The solar electrical fraction can be defined differently depending on whether the household electricity (e.g. lighting, plug loads, and appliances) is considered. If the household electricity is not considered, the metric is called system solar electrical fraction defined as (Zenhäusern 2020):

$$f_{sol,el}^{sys} = \frac{\int E_{PVT}^{AC}\,dt}{\int E_{sys}\,dt} \tag{7}$$

where, E_{PVT}^{AC} is the AC electricity generation (J) from PVT collectors, E_{sys} is the electricity consumed by the system (J). Both items are evaluated every time step.

In contrast, if the household electricity is included, the metric is called site solar electrical fraction defined as (Zenhäusern 2020):

$$f_{sol,el}^{site} = \frac{\int E_{PVT}^{AC}\,dt}{\int (E_{sys} + E_{HE})\,dt} \tag{8}$$

where, E_{HE} is the household electricity consumption (e.g. lighting and appliance).

The system and site solar electrical fractions are presented in Figure 9 for Baltimore and Figure 10 for Las Vegas. Takeaways from these figures are as follows:

- The monthly system solar electrical fraction varied significantly across the year. It changed from 36% (January) to 435% (May) with an annual average of 118% in Baltimore, while it changed from 97% (July) to 746% (November) with a yearly average of 228% in Las Vegas. The values of more than 100% system solar electrical fraction mean that PVT collectors generated more electricity than the consumption by the SAHP system in certain months. The monthly variation is due to the change of solar electricity generation and more importantly the change of electricity

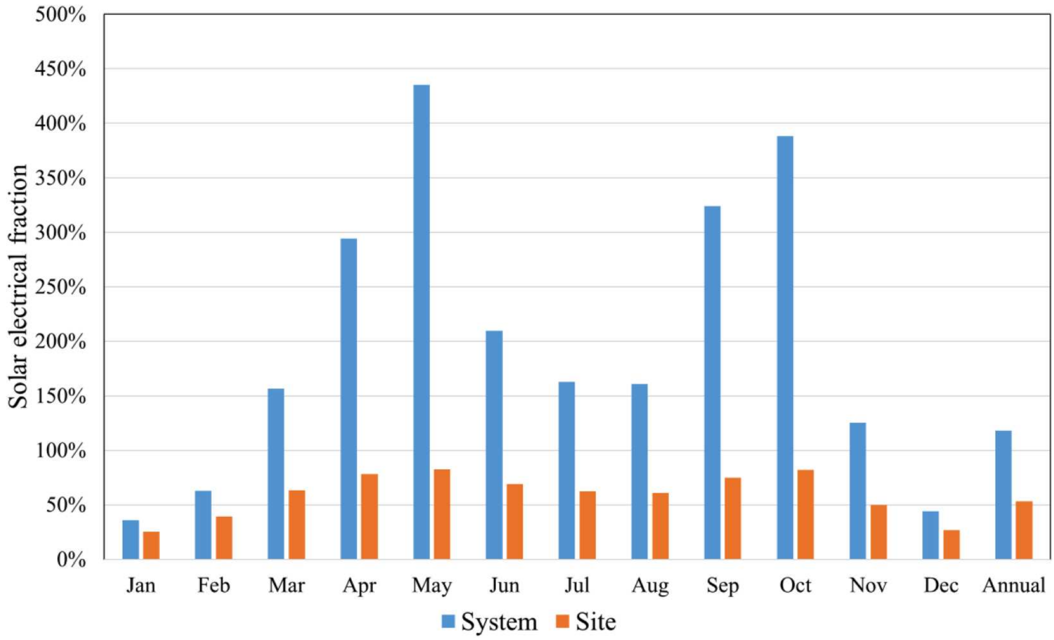

Figure 9. System and site solar electrical fractions in Baltimore.

consumption of the SAHP system. For example, in Baltimore (cold climate), the load for space conditioning increases from the shoulder season, the cooling season, and then the heating season. Therefore, the solar electrical fraction generally increases from the heating season, the cooling season, and then the shoulder season.

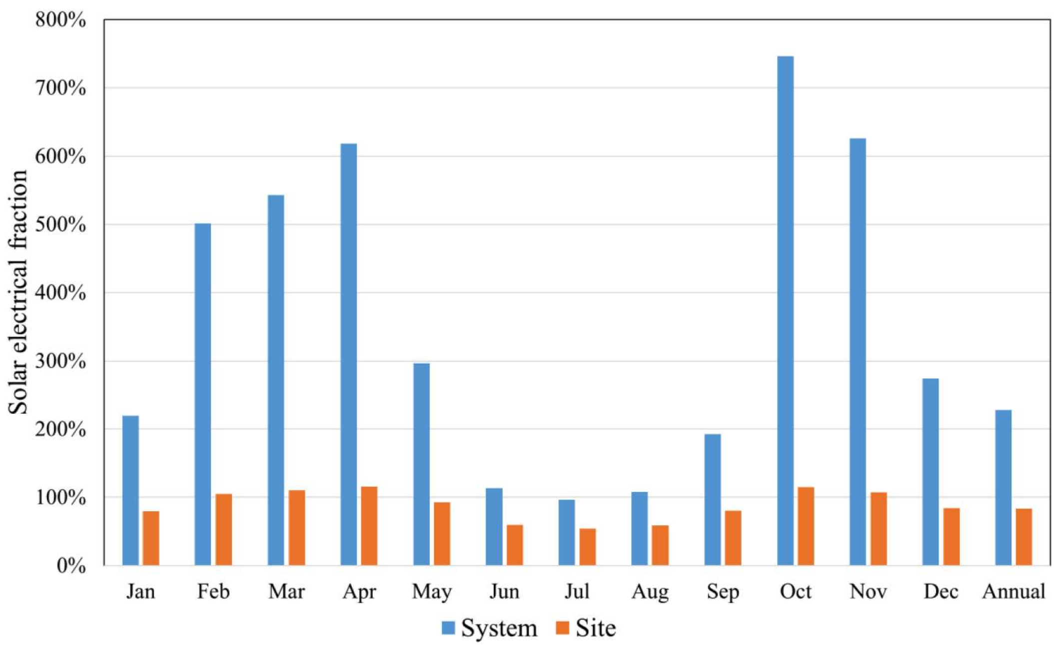

Figure 10. System and site solar electrical fractions in Las Vegas.

- After accounting for the non-HVAC electricity consumption of the building, the site solar electrical fraction took much smaller values than the system solar electrical fraction. The monthly site solar electrical fraction changed from 25% (January) to 83% (May) with an annual average of 53% in Baltimore, while it changed from 54% (July) to 115% (November) with a yearly average of 83% in Las Vegas.

5.5. Electricity cost savings

Table 5 shows the cost items used to calculate annual electricity cost savings of the PVT-based SAHP system relative to the reference ASHP system. In this table, the annual electricity consumption used for space heating and cooling, DHW, lighting, appliance, and plug loads, and the annual electricity generation of PVT collectors are from the TRNSYS simulation outputs. The state average electricity price is for the year 2022 (EIA 2024). The annual electricity cost savings are calculated to be \$1615 in Baltimore and \$1683 in Las Vegas. Based on the annual electricity cost savings, the maximum acceptable total capital cost difference ($CC_{MaxDiff}$) between the SAHP system and the reference system can be calculated as:

$$CC_{MaxDiff} = \frac{AEC*SPP}{1 - PercentCredit} \tag{9}$$

Where, *AEC* is the annual electricity savings (\$), *SPP* is the simple payback period in years, and *PercentCredit* is the incentives in percentage of the capital cost. For example, based on the current federal residential solar tax credit of 30% in the US and a required simple payback period of 5 years, the maximum acceptable total capital cost difference between the PVT-based SAHP system and the reference system is \$11,540 in Baltimore and \$12,020 in Las Vegas.

6. Sensitivity analysis

PVT collector area and thermal storage tank volume are two important design parameters that could affect the energy performance of SAHPs significantly. The results presented earlier in this chapter are based on the collector area of 30 m^2 and the storage tank volume of 2 m^3. They were thus defined after considering the typical favourable roof area for PVT collector installation and the tank footprint and cost. Therefore, it is worthwhile to perform a sensitivity analysis on collector area and storage tank volume. In addition, the impact of using the heat pump to charge the storage tank is investigated because of their uniqueness in the SAHP system design and operation.

6.1. Impact of the collector area and the storage tank volume

In this sensitivity analysis, the PVT collector area was perturbed from 10 m^2 to 50 m^2 with an interval of 10 m^2, and the storage tank volume was perturbed from 0.5 m^3 to 3.5 m^3 with an interval of 0.5 m^3. All combinations of the collector area and tank volume were simulated to explore their impact on SPF.

Table 5. Annual electricity cost savings of the PVT-based SAHP system.

Item	Baltimore	Las Vegas
Electricity consumption of the house with the reference ASHP system (kWh)	17785	16940
Electricity consumption of the house with the PVT-based SAHP system (kWh)	12550	10865
Electricity generation of PVT collectors (kWh)	6890	9310
State average retail electricity price (cents/kWh)	13.32	10.94
Electricity cost of the house with the reference ASHP system (\$)	2369	1853
Electricity cost of the house with the PVT-based SAHP system (\$)	754	170
Electricity cost savings (\$)	1615	1683

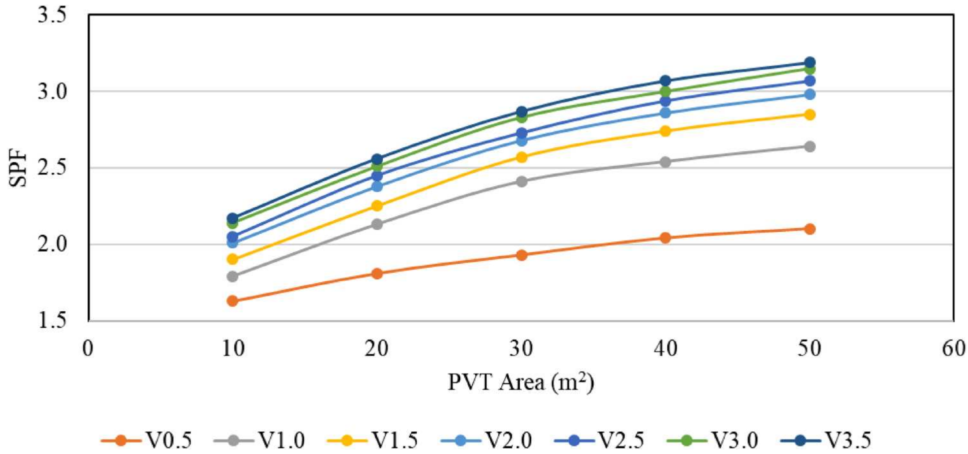

Figure 11. Sensitivity analysis on PVT area and storage tank volume for Baltimore.

Figures 11 and 12 show the results, respectively, for Baltimore and Las Vegas. As expected, the SPF increased with the collector area and the storage tank volume. The SPF tended to saturate at a smaller PVT area as the storage tank volume decreased. For example, in Baltimore, as the collector area increased from 30 m^2 to 50 m^2, the SPF improved slightly for the case of tank volume of 0.5 m^3 but it showed a rapid increase for the case of tank volume of 3.5 m^3. Similarly, the SPF tended to saturate at a smaller tank volume as the collector area decreased. The above observations essentially imply the importance of matching collector area and storage tank volume: a big collector area needs a large tank volume and vice versa.

5.2. Impact of the modes using heat pump to charge the thermal storage tank (Mode 6 and Mode 12)

The intent of using the heat pump to charge the thermal storage for heating (Mode 6) is to increase the storage temperature by using PVT collectors as the source. Increasing the storage temperature improves the capacity and efficiency when the heat pump runs for space heating. Certainly, the use of Mode 6 increases the heat pump running time. Recall that Mode 6 was used in the coldest months

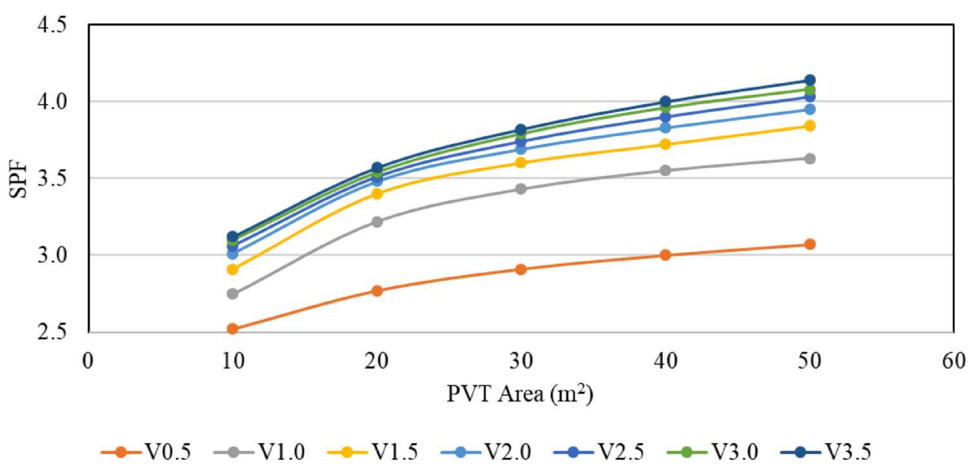

Figure 12. Sensitivity analysis on PVT area and storage tank volume for Las Vegas.

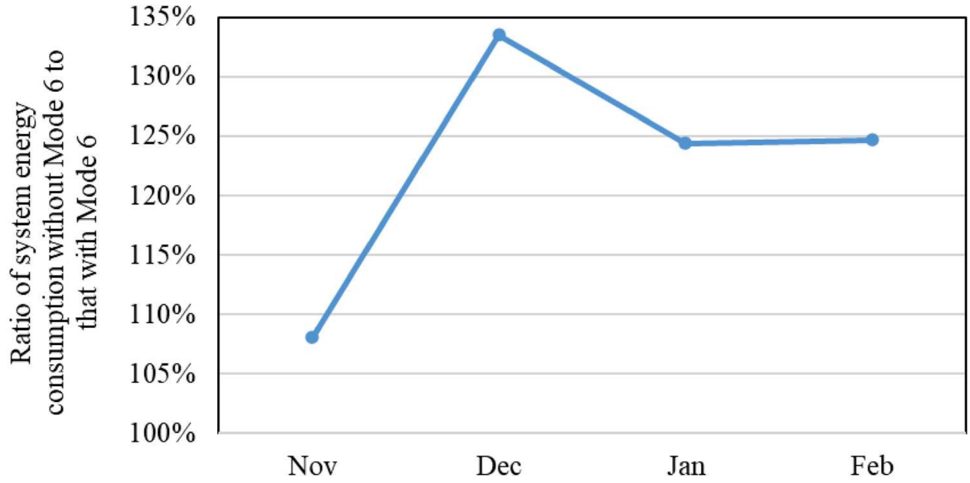

Figure 13. Impact of Mode 6 on the system energy consumption.

(January, February, November, and December) in Baltimore only. The impact of Mode 6 was investigated by deactivating that mode in those four months and comparing the system energy consumption with that prior to the change. Figure 13 shows the results, which indicate that deactivating Mode 6 causes an 8%−34% increase in system energy consumption.

The following scenarios were also investigated: (1) using Mode 6 in March, April, and October in Baltimore; (2) using Mode 6 in December and January in Las Vegas; and (3) using the heat pump to charge the thermal storage for cooling in summer (Mode 12) in both locations. It was found that all the above scenarios could not save energy.

6. Conclusions

The PVT-based SAHP system is distinctive from previous studies because of its multifunctionalities, including onsite electricity generation, space heating, space cooling, and DHW heating. The system has several unique features. First, the PVT collectors are a multi-purpose component of the system. They generate electricity and collect heat energy during the daytime and can work as radiative cooling panels for space cooling. The use of PVT collectors together with the heat pump for space cooling has never been studied in literature to the best of our knowledge. Second, the system has energy cascading features such as using the heat collected from PVT collectors for space heating and DHW and using the desuperheater for DHW production. Third, the mode of using the heat pump to actively charge the thermal storage tank (Mode 6) is a unique feature. The value of this mode in cold climates has been verified with simulations in this work.

The SAHP system has higher SPFs than the reference system throughout the year for both locations. In a cold climate like that of Baltimore, the annual SPF of the SAHP system is 2.69, which is about 70% higher than the reference system. In a warm climate like that of Las Vegas, the annual SPF of the SAHP system is 3.70, which is almost twice as high as the reference system. In addition, the electricity generated by the PVT collectors can cover 53% of the whole building electricity needs in Baltimore and 83% in Las Vegas. These results demonstrate that the climate has dramatic impact on the system performance.

The statistical analysis of the system running time shows that several modes, such as the modes of using PVT collectors directly for space conditioning (Modes 1 and 7) and the mode of using the thermal storage tank directly for space conditioning (Modes 2 and 8) are rarely activated. This means that the system design and sequence of operation can be simplified. Therefore, one avenue of future work is to simplify the system design and operation and investigate its impact on the system performance. The collector tilt angle and critical operating parameters could be included in the sensitivity analysis, or they could be even optimised using a simulation-based optimisation approach. Finally, laboratory testing or field demonstration of the system operation and performance need to be performed in future.

Disclosure statement

No potential conflict of interest was reported by the author(s).

Data availability statement

The data that support the findings of this study are available from the corresponding author, [W.W], upon reasonable request.

References

ASHRAE. 2017. *ASHRAE Handbook: Fundamentals*. Atlanta, GA: The American Society of Heating, Refrigerating, and Air-Conditioning Engineers.

Badiei, A., Y.G. Akhlaghi, X. Zhao, S. Shittu, X. Xiao, J. Li, Y. Fan, and G. Li. 2020. "A Chronological Review of Advances in Solar Assisted Heat Pump Technology in 21st Century." *Renewable and Sustainable Energy Reviews* 132:110132. https://doi.org/10.1016/j.rser.2020.110132

Bakker, M., H.A. Zondag, M.J. Elswijk, K.J. Strootman, and M.J.M. Jong. 2005. "Performance and Costs of a Roof-sized PV/Thermal Array Combined with a Ground Coupled Heat Pump." *Solar Energy* 78 (2): 331–339. https://doi.org/10.1016/j.solener.2004.09.019

Banister, C.J., and M.R. Collins. 2015. "Development and Performance of a Dual Tank Solar-assisted Heat Pump System." *Applied Energy* 149:125–132. https://doi.org/10.1016/j.apenergy.2015.03.130

Besagni, G., L. Croci, R. Nesa, and L. Molinaroli. 2019. "Field Study of a Novel Solar-assisted Dual-source Multifunctional Heat Pump." *Renewable Energy* 132:1185–1215. https://doi.org/10.1016/j.renene.2018.08.076

Cai, J., J. Ji, Y. Wang, and W. Huang. 2016. "Numerical Simulation and Experimental Validation of Indirect Expansion Solar-assisted Multi-functional Heat Pump." *Renewable Energy* 93:280–290. https://doi.org/10.1016/j.renene.2016.02.082

Cai, J., J. Ji, Y. Wang, and W. Huang. 2017. "Operation Characteristics of a Novel Dual Source Multi-functional Heat Pump System under Various Working Modes." *Applied Energy* 194:236–246. https://doi.org/10.1016/j.apenergy.2016.10.075

Chu, J., W. Choi, C.A. Cruickshank, and S.J. Harrison. 2014. "Modeling of an Indirect Solar Assisted Heat Pump System for a High Performance Residential House." *Journal of Solar Energy Engineering* 136 (4): 41003-1– 41003-9.

Del Amo, A., A. Martínez-Gracia, T. Pintanel, A.A. Bayod-Rújula, and S. Torné. 2020. "Analysis and Optimization of a Heat Pump System Coupled to an Installation of PVT Panels and a Seasonal Storage Tank on an Educational Building." *Energy and Buildings* 226:110373. https://doi.org/10.1016/j.enbuild.2020.110373

EIA. 2022. *Total Energy Monthly Data*. U.S. Energy Information Administration. Accessed April 2022. https://www.eia.gov/totalenergy/data/monthly/.

EIA. 2024. *US Electricity Profile 2022*. US Energy Information Administration. Accessed July 2024. https://www.eia.gov/electricity/state/.

Eicker, U., and A. Dalibard. 2011. "Photovoltaic–thermal Collectors for Night Radiative Cooling of Buildings." *Solar Energy* 85 (7): 1322–1335. https://doi.org/10.1016/j.solener.2011.03.015

Entchev, E., L. Yang, M. Ghorab, and E.J. Lee. 2014. "Performance Analysis of a Hybrid Renewable Microgeneration System in Load Sharing Applications." *Applied Thermal Engineering* 71 (2): 697–704. https://doi.org/10.1016/j.applthermaleng.2013.10.057

Evangelisti, L., C. Guattari, and F. Asdrubali. 2019. "On the Sky Temperature Models and their Influence on Buildings Energy Performance: A Critical Review." *Energy and Buildings* 183:607–625. https://doi.org/10.1016/j.enbuild.2018.11.037

Fiorentini, M., P. Cooper, and Z. Ma. 2015. "Development and Optimization of an Innovative HVAC System with Integrated PVT and PCM Thermal Storage for a Net-zero Energy Retrofitted House." *Energy and Buildings* 94:21–32. https://doi.org/10.1016/j.enbuild.2015.02.018

Grossule, F. 2015. "The use of Phase Changing Materials for Cooling of Buildings Combined with Night Sky Radiant Cooling." Master's Thesis. Technical University of Denmark.

Gürlich, D., A. Dalibard, and U. Eicker. 2017. "Photovoltaic-thermal Hybrid Collector Performance for Direct Trigeneration in a European Building Retrofit Case Study." *Energy and Buildings* 152:701–717. https://doi.org/10.1016/j.enbuild.2017.07.081

Hadorn, J.C., ed. 2015. *Solar and Heat Pump Systems for Residential Buildings*. Berlin: Ernst & Sohn.

IECC. 2006. *International Energy Conservation Code*. Washington, DC: International Code Council.

Klein, S.A., W.A. Beckman, J.W. Mitchell, J.A. Duffie, N.A. Duffie, T.L. Freeman, J.C. Mitchell, R.E. Urban, A. Fiksel, et al. 2018. "TRNSYS 18 Mathematical Reference."

Lämmle, M., M. Herrando, and G. Ryan. 2020. Basic Concepts of PVT Collector Technologies, Applications and Markets. Accessed April 2022. https://www.iea-shc.org/Data/Sites/1/publications/IEA-SHC-Task60-D5-Basic-Concepts-of-PVT-Technologies.pdf.

Leonforte, F., A. Miglioli, C. Del Pero, N. Aste, N. Cristiani, L. Croci, and G. Besagni. 2022. "Design and Performance Monitoring of a Novel Photovoltaic-thermal Solar-assisted Heat Pump System for Residential Applications." *Applied Thermal Engineering* 210:118304. https://doi.org/10.1016/j.applthermaleng.2022.118304

Li, Z., and X. Huang. 2022. "Simulation Analysis on Operation Performance of a Hybrid Heat Pump System Integrating Photovoltaic/Thermal and air Source." *Applied Thermal Engineering* 200:117693. https://doi.org/10.1016/j.applthermaleng.2021.117693

Lin, W., Z. Ma, M.I. Sohel, and P. Cooper. 2014. "Development and Evaluation of a Ceiling Ventilation System Enhanced by Solar Photovoltaic Thermal Collectors and Phase Change Materials." *Energy Conversion and Management* 88:218–230. https://doi.org/10.1016/j.enconman.2014.08.019

Ma, J., A.S. Fung, M. Brands, O.M.A. Moyeed, A. Mhanna, and N. Juan. 2021. "Effects of Photovoltaic/Thermal (PV/T) Control Strategies on the Performance of Liquid-based PV/T Assisted Heat Pump for Space Heating." *Renewable Energy* 172:753–764. https://doi.org/10.1016/j.renene.2021.02.030

Martin, M., and P. Berdahl. 1984. "Characteristics of Infrared Sky Radiation in the United States." *Solar Energy* 33 (3–4): 321–336. https://doi.org/10.1016/0038-092X(84)90162-2

Martinez-Gracia, A., J. Uche, A. del Amo, A.A. Bayod-Rujula, S. Uson, and I. Arauzo. 2022. "Energy and Environmental Benefits of an Integrated Solar Photovoltaic and Thermal Hybrid, Seasonal Storage and Heat Pump System for Social Housing." *Applied Thermal Engineering* 213:118662. https://doi.org/10.1016/j.applthermaleng.2022.118662

Miglioli, A., N. Aste, C. Del Pero, and F. Leonforte. 2023. "Photovoltaic-thermal Solar-Assisted Heat Pump Systems for Building Applications: Integration and Design Methods." *Energy and Built Environment* 4 (1): 39–56. https://doi.org/10.1016/j.enbenv.2021.07.002

Mohanraj, M., Y. Belyayev, S. Jayaraj, and A. Kaltayev. 2018. "Research and Developments on Solar Assisted Compression Heat Pump Systems – A Comprehensive Review (Part-B: Applications)." *Renewable and Sustainable Energy Reviews* 83:124–155. https://doi.org/10.1016/j.rser.2017.08.086

Qu, S., F. Ma, R. Ji, D. Wang, and L. Yang. 2015. "System Design and Energy Performance of a Solar Heat Pump Heating System with Dual-Tank Latent Heat Storage." *Energy and Buildings* 105:294–301. https://doi.org/10.1016/j.enbuild.2015.07.040

Simonetti, R., L. Moretti, L. Molinaroli, and G. Manzolini. 2020. "Energetic and Economic Optimization of the Yearly Performance of Three Different Solar Assisted Heat Pump Systems Using a Mixed Integer Linear Programming Algorithm." *Energy Conversion and Management* 206:112446. https://doi.org/10.1016/j.enconman.2019.112446

Sterling, S.J., and M.R. Collins. 2012. "Feasibility Analysis of an Indirect Heat Pump Assisted Solar Domestic Hot Water System." *Applied Energy* 93:11–17. https://doi.org/10.1016/j.apenergy.2011.05.050

Vallati, A., P. Ocłoń, C. Colucci, L. Mauri, R. de Lieto Vollaro, and J. Taler. 2019. "Energy Analysis of a Thermal System Composed by a Heat Pump Coupled with a PVT Solar Collector." *Energy* 174:91–96. https://doi.org/10.1016/j.energy.2019.02.152

Wang, Q., Y.Q. Liu, G.F. Liang, J.R. Li, S.F. Sun, and G.M. Chen. 2011. "Development and Experimental Validation of a Novel Indirect-expansion Solar-assisted Multifunctional Heat Pump." *Energy and Buildings* 43 (2–3): 300–304. https://doi.org/10.1016/j.enbuild.2010.09.013

Zare, A. 2021. "Design, Simulation, and Performance Analysis of Multifunctional Solar-assisted Heat Pump Systems for Residential Buildings." Ph.D. Dissertation, The University of North Carolina at Charlotte.

Zenhäusern, D. 2020. *Key Performance Indicators for PVT Systems*. Accessed April 2022. https://www.iea-shc.org/Data/Sites/1/publications/IEA-SHC-Task60-D1-Key-Performance-Indicators.pdf.